THE ASTROPHYSICAL JOURNAL, 230:526–533, 1979 June 1

BALLOON-BORNE ULTRAVIOLET STELLAR SPECTROGRAPH. I. INSTRUMENTATION AND OBSERVATION

Y. KONDO,* C. DE JAGER,† R. HOEKSTRA†, K. A. VAN DER HUCHT,† T. M. KAMPERMAN,†
H. J. G. L. M. LAMERS,† J. L. MODISETTE,‡ AND T. H. MORGAN‡

Received 1978 June 26; accepted 1978 December 8

ABSTRACT

A Balloon-borne Ultraviolet Stellar Spectrograph (BUSS), featuring a dual star-tracking system and a system comprising a telescope, an echelle spectrograph, and an SEC vidicon, was successfully flown twice in 1976 and twice in 1978. In total, 81 spectra of 56 stars were recorded in the wavelength range from 2200 to 3400 Å with resolution of 0.1 Å.

In this article, we present a description of the instrumentation, its operation, observations obtained, and other relevant matter relating to the BUSS flights. In the companion article, we present highlights of the observational results.

Subject headings: instruments — ultraviolet: spectra

I. INTRODUCTION AND INSTRUMENTATION

The current Balloon-borne Ultraviolet Stellar Spectrograph (BUSS) is the result of a collaboration among the NASA Johnson Space Center at Houston, the Space Research Laboratory at Utrecht, and Houston Baptist University. Prior to this collaborative effort, four scientific data flights were successfully conducted with instrumentation developed by Ball Brothers Research Corporation under the direction of the BUSS project team at the Johnson Space Center and Houston Baptist University (Kondo *et al.* 1972). In 1975 the Ebert-Fastie spectrometer and image-dissector tube were replaced by an echelle spectrograph and an SEC vidicon developed at the Space Research Laboratory. The instrument is capable of recording the spectra of stars with a visual magnitude brighter than 6 (depending on the spectral type) in the wavelength range from 2000 to 3400 Å with a resolution of 0.1 Å. In 1976, and again in 1978, two scientific data flights were successfully carried out with the new BUSS payload from Palestine, Texas. A total of 81 spectra were recorded of 56 stars. In de Jager *et al.* 1979, hereafter Paper II, highlights of the observational results are presented.

Table 1 summarizes the instrumental characteristics and Figure 1 shows the schematic of the optical system. For a detailed description of the new payload, see Hoekstra *et al.* (1978).

II. OPERATION OF THE PAYLOAD

In order to obtain a large number of spectra during single nights of observations, both the instrument and the project organization have to be optimized for maximum speed of operation.

The instrument itself is very fast, using: (*a*) a slitless spectrograph, which requires thermally very stable accurate pointing; (*b*) an integrating detector system, which simultaneously accumulates photons at all wavelengths with high quantum efficiency; and (*c*) high-quality reflective coatings for the ultraviolet.

The project organization during the flights is such that: (*a*) scientific and instrument housekeeping data are checked at two separate consoles; (*b*) the activities concerning balloon position, ballast, etc., are totally independent of the scientific payload operations; (*c*) the navigation of the payload is done in parallel with the readout of data from the camera tube and its preparation for the next observation; (*d*) accurate calibration parameters of the pointing loops speed up the star acquisition process; and (*e*) the astronomers have a display of quick-look scientific data, which enables continual optimization of the observational program.

The last capability enables the scientist to judge the quality of the data and to check the spectra for unexpected features. On the basis of this information real-time decisions on the observing program can be made fruitfully, especially those related to the choice of the exposure times and repeated observations of particularly interesting objects. Figure 2 gives a diagram of the activities between the end of one exposure and the beginning of the next exposure of another star. At least 15 telecommands have to be transmitted to the instrument and the platform. With the recently developed software-controlled command-generation system the minimum cycle time of 8½ minutes as indicated in the diagram was actually achieved during the BUSS IX and X flights; in the past, cycle times of 15 minutes were typical. (When faint stars in the Milky Way are to be observed, the verification of the proper target does take extra time.) The combination of the short cycle time and the short exposure times allows the observation of a large number of spectra during one night.

* NASA Goddard Space Flight Center.
† Space Research Laboratory, Utrecht, The Netherlands.
‡ Houston Baptist University.

TABLE 1

BUSS TECHNICAL DATA SUMMARY

Telescope (NASA, JSC):	
Type	Ritchey-Chrétien f/7.5
Diameter	40 cm
Focal length	300 cm
Image quality	1.″2 (90% energy)
Pointing (NASA, JSC):	
Coarse pointing	1° (magnetometer + potentiometer)
Fine pointing	2′ (outer loop star-tracker)
Fine guidance	2″ (inner loop star-tracker)
Spectrograph (SRL):	
Echelle	79 gr mm^{-1}; 63° blaze angle (Bausch & Lomb)
Spectral range	2000–3400 Å
Spectral orders	112–66
Collimator	f = 523 mm, f/7.5 off-axis
Prism	Fused silica, 15° top angle
Catadioptric imaging system	f = 510 mm, f/4.5
Transmission	7.4% (dichroid + spectrograph at 2537 Å)
Aperture	1′ (circular field)
Detector (SRL):	
TV camera	SEC vidicon (Westinghouse WX31718)
Photocathode	CsTe on MgF_2 window
Sensitive area	25 mm square format
Secondary gain	50–100
Scan raster	1024 × 1024 pixels
Line scan time	20 ms
Performance	
Resolving power	3×10^4

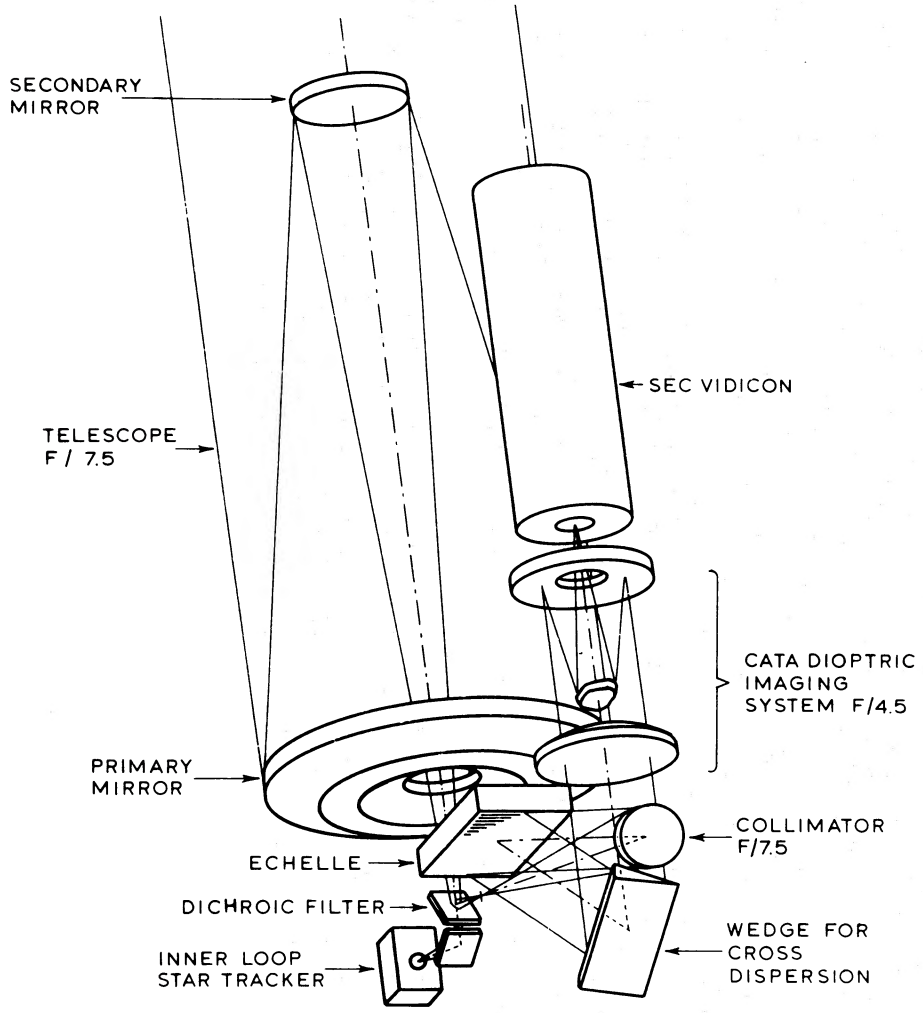

FIG. 1.—A schematic of the BUSS optical system

III. OBSERVATIONS

The stars observed in the 1976 and 1978 flights are listed in Tables 2A and 2B, respectively, arranged by spectral type, together with relevant information. The two successful flights in 1976 were held on the nights of May 16/17 and September 19/20. In these two flights 53 spectra of 33 stars were obtained. The third and fourth data flights took place on the nights of 1978 May 8/9 and May 30/31; 28 spectra of 23 stars were obtained. The program stars were selected on the basis of astrophysical interests, considering observational constraints, such as integration time, magnitude, launch date, etc.

A large fraction of the stars were observed with both a short and a long exposure. The long exposure is needed to obtain a good signal-to-noise ratio in the wavelength region of 2400–2600 Å, where the residual ozone in the Earth's atmosphere absorbs about 70% to 80% of the flux. Observations of α Boo and ζ Oph in the spectral region of the Mg II resonance doublet near 2800 Å are shown as examples in Figures 3 and 4. The data presented are uncalibrated observations in the form monitored by the scientists during the flight operation. For a well-exposed spectrum the noise is typically about 2% (rms). (See also the next section). In Figure 5 we show a part of the calibrated spectrum of α CMi which demonstrates the high spectral resolution of 0.1 Å.

IV. CALIBRATION

a) Wavelength Calibration

Although the overall spectral resolution of BUSS is 0.1 Å, it is possible to localize the centers of spectral lines with a much greater accuracy. In undisturbed lines with high signal-to-noise ratios, spectral lines can be localized with an accuracy of 0.01 Å. Accordingly, our aim is to attain that accuracy in wavelength determination, where feasible.

Prior to the flights, calibration spectra were recorded by using the emission lines of hollow-cathode light sources as wavelength references. From these measurements, empirical dispersion relations were established for all spectral orders, relating the wavelengths of spectral lines to their positions in the output image of the detector. Linear functions with cubic corrections at both ends of the spectral orders for compensating detector deformations were found adequate to yield the required 0.01 Å accuracy for those spectral orders where a sufficient number of standard lines were available. However, for the spectral orders with only a few standard lines (especially in the wavelength range shortward of 2500 Å), the parameters of the dispersion relations could not be fitted uniquely to the standards. Nevertheless, the relations obtained enabled us to identify many thousands of spectral lines in stellar BUSS observations. In particular, more than 2000 lines were identified in the BUSS spectrum of Procyon. Because the density of these lines was much higher than that of the preflight calibration lines, we have readjusted the dispersion parameters for all spectral orders to the set of identified lines in the Procyon spectrum. This yielded our final wavelength scale, to which were added corrections for differential Doppler effects and for the influence of the Earth magnetic field on the detector. The wavelength accuracy obtained in this way for Procyon is approximately 0.01 Å for undisturbed spectral lines. The wavelength scale for other BUSS observations is less accurate, due partially to the fact that the magnetic shifts are known with an accuracy of half a pixel only, but primarily due to the fact that the radial velocities of stars are variable in many cases. However, the wavelength uncertainties resulting from this are systematic and will seldom exceed 0.1 Å.

b) Efficiency Calibration

The objective here is to transform the detector signals, $S(\lambda)$, into stellar fluxes, $F(\lambda)$. The relation between $F(\lambda)$ and $S(\lambda)$ is rather complicated, because so many different effects intervene. Some of these are simply dependent on wavelength only, such as reflection and transmission coefficients of most of the optical components and the residual ozone absorption, but the optical efficiency of the echelle grating is dependent both on wavelength and on spectral order. Finally, the detector is the most complicated link in the chain connecting $F(\lambda)$ with $S(\lambda)$: in principle, all pixels have their own nonlinear curves.

The detector calibration is described below in § IV*c*. By using a calibrated UV deuterium lamp as a light source in the laboratory, we were able to determine the global relative instrument sensitivity as a function of wavelength. The result is shown in Figure 6. The data points in the figure correspond to the signals obtained in the centers of the spectral orders of the echelle. Moreover, the detector calibration described below was applied in order to remove detector nonlinearity and sensitivity changes over the detector's sensitive area. The curve of Figure 6 represents the product of efficiencies of the optical components involved, and the quantum efficiency of the SEC vidicon photocathode. The bumpy appearance of the curve is due to the reflection characteristics of the multilayer dichroic filter, while the rapid decrease of the relative sensitivity toward longer wavelengths is due to the rapid falloff of the quantum efficiency of the solar-blind detector photocathode.

The data presented in Figure 6 were obtained by studying $S(\lambda)$ in the centers of the spectral orders. When we stay inside one order, and study the relative sensitivity along the order from one end to the other, we expect to find the $\sin^2/\phi^2$ curve characteristic for blazed gratings. Figure 7 displays a relative sensitivity curve for order 80 as was deduced from the BUSS observation of the star ζ Oph. A flat $F(\lambda)$ was assumed and also, in this case, the detector calibration was applied to remove the detector influences. Moreover, a correction was applied for removing the influence of the rapidly changing transmission of the residual ozone.

The in-flight behavior of the BUSS efficiency is still being investigated. It is our intention that in the final

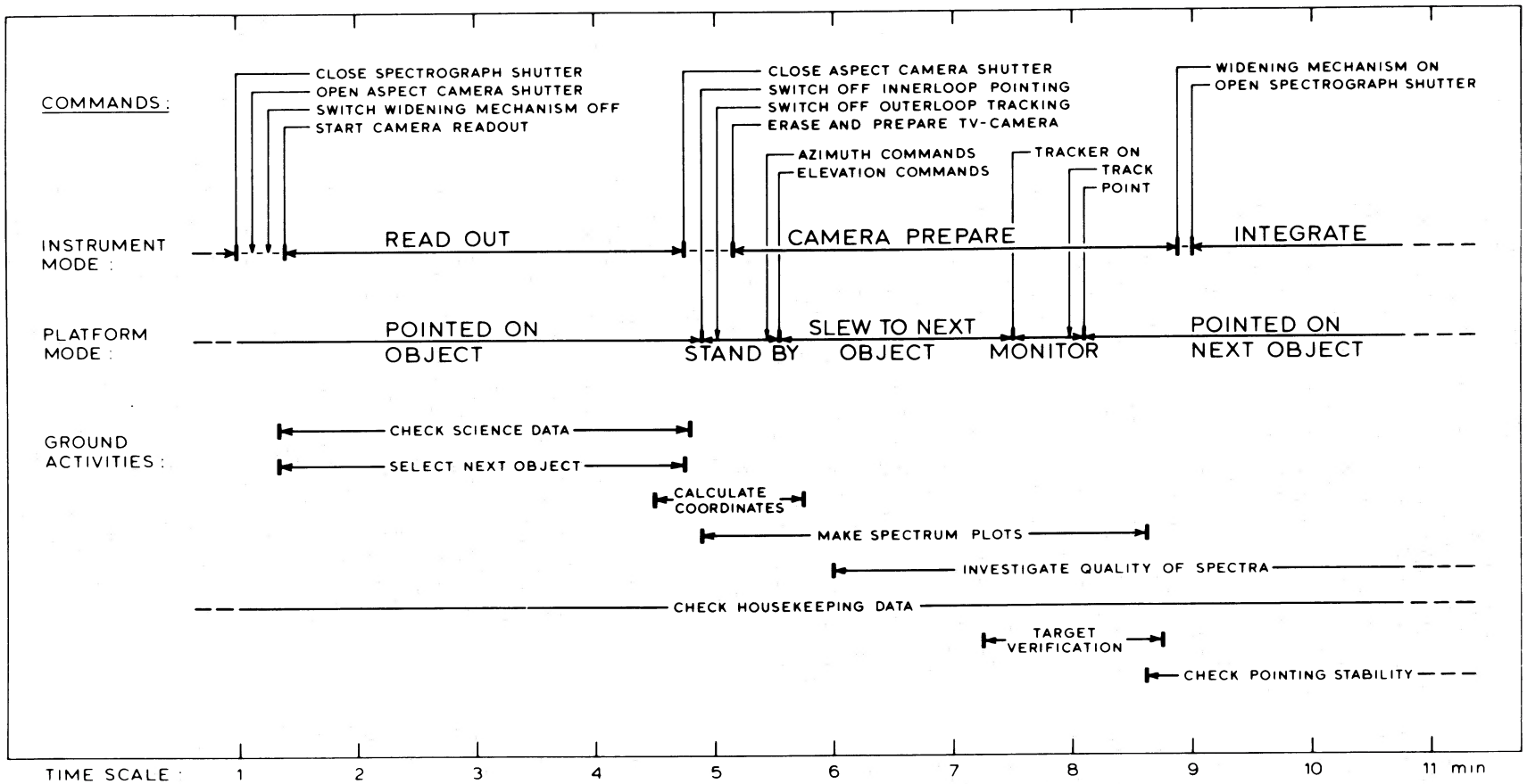

FIG. 2.—BUSS operations timing diagram

TABLE 2A

BUSS VII (1976 May 20 UT) + BUSS VIII (1976 Sep 17 UT) OBSERVATIONS

HR	Star Name	Name	Sp. Type		m_v	Number of Observations	Integration Time
1.....	6175	ζ Oph	O9.5	V	2.56	VII2	4 min, 20 min
2.....	264	γ Cas	B0.5	IVe	2.65	VIII2	1.5 min, 4 min
3.....	4133	ρ Leo	B1	Ib	3.85	VII2	4 min, 11 min
4.....	6084	σ Sco	B1	III	2.93	VII1	8 min
5.....	496	φ Per	B1	III–V? pe	4.03	VIII1	7 min
6.....	5056	α Vir	B1	V	0.96	VII4	15 s, 30 s, 30 s, 5 min
7.....	1552	π Ori	B2	III	3.69	VIII1	6 min
8.....	8238	β Cep	B2	III	3.30	VII2, VIII2	1 min, 5 min, 5 min, 3 min
9.....	39	γ Peg	B2	IV	2.83	VIII3	2 min, 7 min, 2 min
10.....	8146	μ Cyg	B2	Ve	4.45	VIII7	10 min
11.....	6588	ι Her	B3	V	3.80	VII2, VIII7	4.5 min, 12 min, 20 min
12.....	1910	ζ Tau	B4	IIID	2.70	VIII1	8 min
13.....	6714	67 Oph	B5	Ib	3.97	VII1	4 min
14.....	6396	ζ Dra	B6	III	3.20	VIII2	13 min, 5 min
15.....	8762	ο And	B6	p	3.60	VIII1	10 min
16.....	7106	β Lyr	B	pe	3.43	VII1	10 min
17.....	4662	γ Crv	B8	IIIp	2.60	VII1	24 min
18.....	1713	β Ori	B8	Ia	0.08	VIII2	40 s, 8 min
19.....	15	α And	B9	IIIp	2.06	VIII1	4 min
20.....	3975	η Leo	A0	Ib	3.48	VII1	30 min
21.....	7001	α Lyr	A0	V	0.04	VII2	26 s, 8 min
22.....	7924	α Cyg	A2	Ia	1.26	VII1, VIII1	15 min, 5 min
23.....	7557	α Aql	A7	V	0.77	VIII2	15 min, 4 min
24.....	1605	ε Aur	A8	Ia	2.99	VIII1	25 min
25.....	7377	δ Aql	F0	IV	3.36	VIII1	10 min
26.....	1017	α Per	F5	Ib	1.78	VIII1	20 min
27.....	2943	α CMi	F5	IV	0.34	VIII2	3 min, 10 min
28.....	424	α UMi	F8	Ib	2.5	VII1	6.7 min
29.....	1708	α Aur	G8	III + F	0.09	VIII2	15 min, 5 min
30.....	5340	α Boo	K2	IIIp	0.2	VII1	35 min
31.....	1457	α Tau	K5	III	0.86	VIII1	15 min
32.....	6134	α Sco	M1.5	Iab + B2.5 V	1.08	VII1	45 min
33.....	2061	α Ori	M2	Iab	0.80	VIII1	15 min

TABLE 2B

BUSS IX (1978 May 9 UT) + BUSS X (1978 May 31 UT) OBSERVATIONS

	HR	Star Name	Sp. Type	m_v	Number of Observations	Integration Time
1.....	8469	λ Cep	O6 f	5.04	X 1	45 min
2.....	7763	P Cyg	B1 Iape	4.83	X 1	30 min
3.....	6118	χ Oph	B1.5 IVe	4.43	IX 1	13 min
4.....	8047	59 Cyg	B1.5 IVe	4.75	IX 1	10 min
5.....	6787	102 Her	B2 V	4.35	IX 1	12 min
6.....	6112	ρ Oph	B3 V	4.63	IX 1	12 min
7.....	6588	ι Her	B3 V	3.80	IX 1	8 min
8.....	5941	48 Lib	B5 IIIp	4.87	IX 1, X1	10 min, 39 min
9.....	4787	κ Dra	B6 IIIp	3.89	IX 1	16 min
10.....	8762	ο And	B6p	3.62	IX 1	12 min
11.....	3982	α Leo	B7 V	1.35	IX 3	2 min, 6 min, 3 min
12.....	6812	μ Sgr	B8 Iab	3.85	IX 1	14 min
13.....	4915	α^2 CVn	B9.5p	2.89	IX 1	6 min
14.....	7342	υ Sgr	Apep	4.58	X 1	60 min
15.....	4295	β UMa	A1 V	2.36	X 1	10 min
16.....	5054	ζ UMa	A2 V	2.06	IX 1	7 min
17.....	8378	η Oph	A2.5 V	2.44	X 1	15 min
18.....	0021	β Cas	F2 IV	2.24	X 1	35 min
19.....	4968	α Com	F5 V	4.32	IX 1	30 min
20.....	5933	γ Ser	F6 IV	3.86	IX 2	5 min, 35 min
21.....	5338	ι Vir	F7 IV	4.07	X 1	60 min
22.....	4540	β Vir	F8 V	3.61	X 1	60 min
23.....	6536	β Dra	G2 II	2.78	IX 1	10 min
24.....	4301	α UMa	K0 II–III	1.79	IX 1	11 min

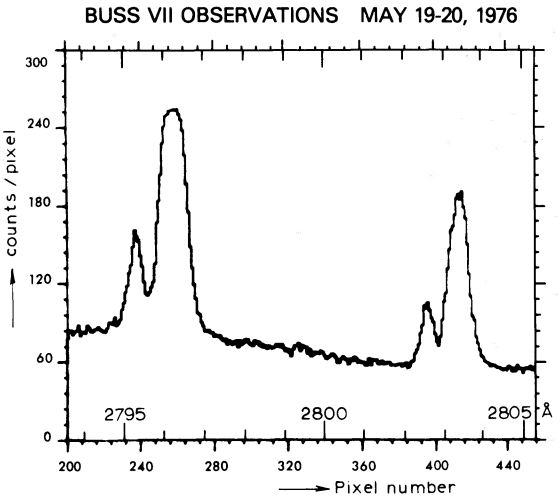

FIG. 3.—Mg II resonance lines in the BUSS VII spectrum of α Boo (K2 IIIp): Raw, uncalibrated quick-look data.

presentation of the BUSS observations the influences of optical efficiencies, grating blaze, and detector be removed.

c) *Detector Calibration*

The photometric behavior of the SEC camera was determined as mentioned above during preflight calibrations by recording the detector response resulting from a constant and uniform UV photocathode illumination. A deuterium lamp was used with a 2537 Å interference filter at about 1 m distance from the camera window. A sequence of 10 different exposure times was used, and each exposure of a given time was recorded on digital tape—a total of more than hundred million numbers!

Several procedures to correct for the sensitivity curves for all individual pixels of the detector have been worked out.

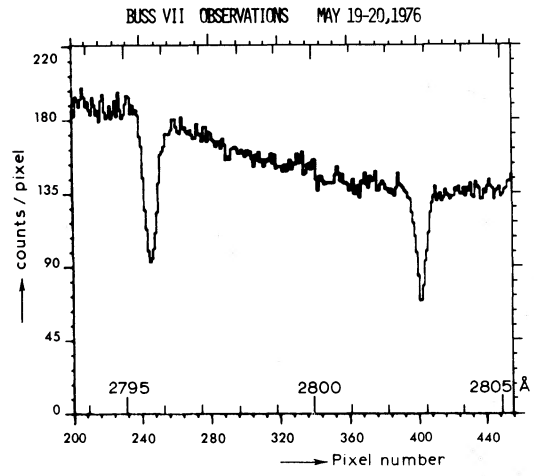

FIG. 4.—Mg II resonance lines in the BUSS VII spectrum of ζ Oph (O9.5 V): Raw, uncalibrated quick-look data.

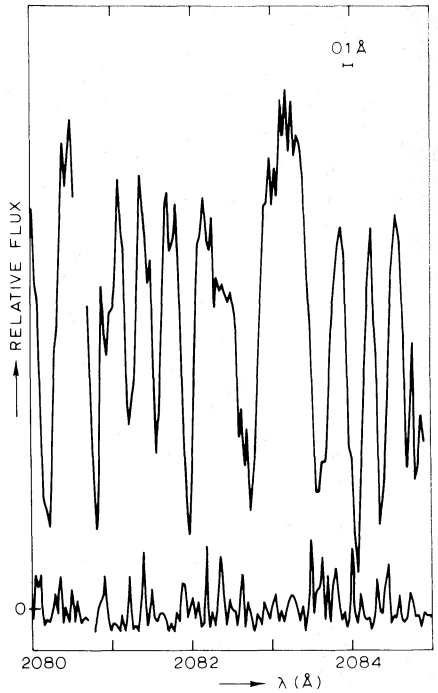

FIG. 5.—Part of the calibrated BUSS VIII spectrum of α CMi (F5 IV–V) which shows that a spectral resolution of 0.1 Å is achieved.

The following effects have to be taken care of: (*a*) The quantum efficiency of the tube varies over the photocathode area. (*b*) The gain of the tube is a function of the potential across the target. This potential changes with the amount of charge accumulated and with the geometry of the deflection yokes, readout beam, etc. (*c*) On a small scale, variations in efficiency can occur between individual pixels. This appears to be related to the grainy structure of the target.

The first two effects are calibrated out by a procedure similar to the one described by Crane (1973), in which sensitivity curves averaged over 4 × 4 pixel areas are interpolated. Currently two alternatives are being investigated: (*a*) representation of the individual curves on a log-log scale, and (*b*) fitting the curves with fifth-order polynomials. For final processing of the data obtained, the most efficient routines will be chosen. The third effect, the so-called fixed pattern noise, is taken care of separately. Due to the small scale of this effect (50–100 μm) the shift of the echellograms due to the influence of the Earth's magnetic field has to be removed first. This is accomplished by a computer routine which shifts the echellograms in such a way that the target blemishes in the flight spectra coincide with the same blemishes from the preflight recordings. After that the pixel is individually treated for its sensitivity relative to the mean sensitivity in the 4 × 4 pixel area for which the complete curve is applied. The average deviation from the mean sensitivity is 3½%. In a "properly" exposed spectrum the noise contribution from the statistical error in the number of photoelectrons gathered per resolution

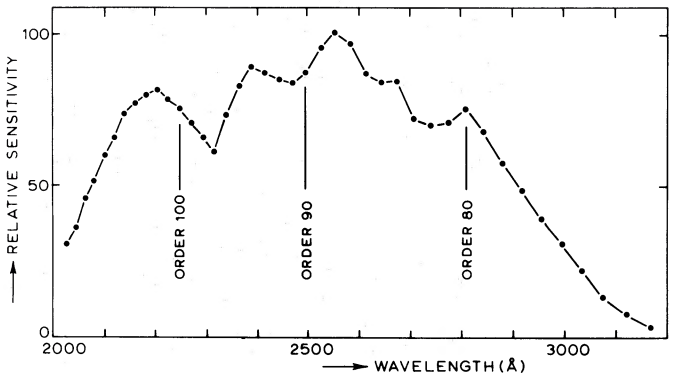

FIG. 6.—The global relative sensitivity of BUSS as a function of wavelength. The results are deduced from preflight calibration measurements. The data points correspond to the centers of the spectral orders.

element is much larger than the contributions from beam shot noise, preamplifier noise, and digitizing noise. Theoretically a value below 1½% noise (rms) could be achieved. Residuals of the fixed pattern noise and the intensity calibration itself, however, degrade this best achievable value to a typical value of 2% noise (rms). At a level of one-fifth of "proper" exposure, e.g., at about 1500 photoelectrons per resolution element, the statistical noise equals the detector noise, but the total is still only 5% (rms).

V. RESIDUAL OZONE ABSORPTION

Determination of the absorption due to the residual ozone above the balloon float altitude of about 40 km is a complex problem. The absorption depends critically on the altitude and the zenith angle; it may also depend on the geographic location and the time (in terms of the day or the season) of observation. The payload does NOT float at the same altitude and a plane-parallel model is probably inadequate to describe the density distribution in the atmosphere. Since these factors vary from one observation to another, a simple evaluation of "the" extinction is not feasible. In fact, the optimum integration time for an object changes significantly during a flight. However, useful stellar spectra can be obtained in the region of 2550 Å by lengthening the integration time by a factor of 3 to 5 compared with that for the region around 2300 and 2800 Å. For an earlier estimate of the extinction in this spectral range, the reader is referred to, for instance, Navach, Lehmann, and Hugenin (1973). The BUSS observations do not show any structure in the ozone absorption band on a wavelength scale shorter than 10 Å (at an accuracy level of 5% to 7%).

VI. CONCLUDING COMMENTS

A balloon-borne spectrograph can be an effective tool for studying the mid-ultraviolet stellar spectrum. A balloon-borne telescope also provides an opportunity for testing and implementing state-of-the-art astronomical instrumentation in a short time frame at a relatively modest cost. We are currently planning to improve the resolving power ($\lambda/\Delta\lambda$) of the BUSS payload to 100,000.

The observations obtained in the BUSS project are being made available to interested scientists primarily on a cooperative basis. Those interested are cordially invited to get in touch with either Y. Kondo or C. de Jager.

We wish to express our sincere appreciation to the following individuals for their contribution to the engineering development of the current BUSS payload and its operation: In the USA, Messrs. C. Craddock, D. Teegarden, and D. White of JSC; Messrs. T.

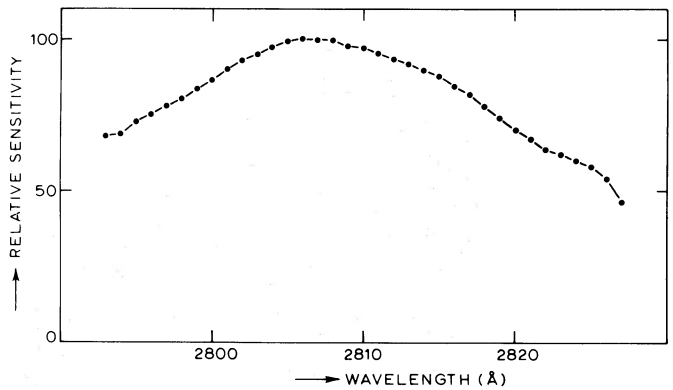

FIG. 7.—The relative sensitivity of BUSS for spectral order 80. The result was deduced from the observed spectrum of ζ Oph.

Doebbler, F. Gaudiano, P. Huddock, C. Laird, G. Teasley, H. Vordenbaum, and C. Wells (team leader) of Lockheed Electronic Corporation at JSC, and Ray S. Whaley and J. McDonnold, students at Houston Baptist University. In the Netherlands, Messrs. T. d'Arnaud, L. van den Brink, W. Van Dijkhuizen, P. de Groene, M. van der Linden, A. Maas, Z. van der Meij, and F. Werkhoven, assisted by E. van der Berg, J. Veenendaal, and J. Hoofd, all of SRL, and Drs. W. Werner, W. Lock, and Messrs. A. van Valkenburg and K. Moddemyer of TPD. We also thank the personnel of the NCAR balloon base at Palestine, Texas, for their competent support in flight operations. The University of Brussels and the University of Mons, Belgium, contributed financially to the 1978 BUSS flights; C. de Loore, L. Houziaux, and their co-workers at these universities are participating in research using the BUSS observations.

REFERENCES

Crane, P. 1973, in *Astronomical Observations with Television-type Sensors*, ed. J. W. Glaspey and G. A. H. Walker (Vancouver: Institute of Astronomy and Space Science), p. 391.

de Jager, C. Kondo, Y., Hoekstra, R., van der Hucht, K. A., Kamperman, T., Lamers, H. J., Modisette, J. L., and Morgan, T. H. 1979, *Ap. J.*, **230**, 534.

Hoekstra, R., Kamperman, T. M., Wells, C. W., and Werner, W. 1978, *Appl. Optics*, **17**, 604.

Kondo, Y., Giuli, T. R., Modisette, J. L., and Rydgren, A. E. 1972, *Ap. J.*, **176**, 153.

Navach, C., Lehmann, M., and Huguenin, D. 1973, *Astr. Ap.*, **22**, 361.

C. DE JAGER, R. HOEKSTRA, T. M. KAMPERMAN, H. J. G. L. M. LAMERS, and K. A. VAN DER HUCHT: Space Research Laboratory, Beneluxlaan 21, Utrecht, The Netherlands

Y. KONDO: Code 685, NASA Goddard Space Flight Center, Greenbelt, MD 20771

J. L. MODISETTE and T. H. MORGAN: Houston Baptist University, 7502 Fondren Road, Houston, TX 77074

THE ASTROPHYSICAL JOURNAL, 230:534–539, 1979 June 1

BALLOON-BORNE ULTRAVIOLET STELLAR SPECTROGRAPH. II. HIGHLIGHTS OF FIRST OBSERVATIONAL RESULTS

C. DE JAGER,* Y. KONDO,† R. HOEKSTRA,* K. A. VAN DER HUCHT,* T. M. KAMPERMAN,* H. J. G. L. M. LAMERS,* J. L. MODISETTE,‡ AND T. H. MORGAN‡

Received 1978 June 26; accepted 1978 December 8

ABSTRACT

We describe a few of the most important features, visible in a first inspection of the high-resolution (0.1 Å) mid-ultraviolet spectra (2000–3250 Å) of 33 stars obtained in two BUSS flights. The profiles of the Mg II lines in early-type (B8–A2) supergiants show the existence of considerable mass flow, partly in irregular "puffs." The features in Mg II in Betelgeuse are due to a cool expanding outer shell above a hotter chromospheric region. Emission features in the shell star ζ Tau indicate infalling material, while the Be star ϕ Per has a mass outflow. We have detected some 80 emission lines of Fe I, Fe II, and Fe III in spectra of late-type giants and supergiants. The composite spectrum of the binary α Sco (M1.5 Iab + B2.5 V) is described, with particular reference to circumstellar lines.

Subject headings: line identifications — stars: Be — stars: mass loss — stars: supergiants — ultraviolet: spectra

I. INTRODUCTION

During its flights on 1976 May 19/20 and September 16/17 the Balloon-borne Ultraviolet Stellar Spectrograph (BUSS) secured 53 high-resolution (0.1 Å) spectra of 33 stars in the spectral range 2000–3250 Å. The instrument and its performance are described in the preceding paper (Kondo *et al.* 1979, hereafter Paper I).

In this paper we summarize a few of the results obtained from first inspections of the rich observational material. Our summary refers chiefly to ultraviolet Mg II lines and some inferences drawn from these lines regarding mass loss, and to chromospheric or shell-type phenomena around giants and supergiants. We also describe spectra of a few Be stars and a shell star.

II. THE Mg II LINES IN LATE-B AND A-TYPE SUPERGIANTS

The most sensitive indicators of mass loss from O and early-B supergiants are the far-ultraviolet resonance lines of C IV, N V, and Si IV. In the cooler A and F supergiants the degree of ionization is lower, and so in such stars the Mg II and Fe II resonance lines in the mid-ultraviolet spectral region are more sensitive indicators of mass loss. In Figure 1 we show the Mg II profiles of the three supergiants β Ori (B8 Ia), η Leo (A0 Ib), and α Cyg (A2 Ia) observed by BUSS. The spectrum of α Lyr (A0 V) is included for a comparison between the supergiants and a main-sequence star.

The resonance lines in α Cyg are very wide and shifted to shorter wavelengths. The short-wavelength side has a steep edge at -250 km s^{-1}. The long-wavelength side shows a less steep increase in flux from -150 km s^{-1} to $+50$ km s^{-1} with a sharp interstellar component at 0 km s^{-1} superposed on it. These profiles resemble the P Cygni profiles of the N V resonance lines in O stars observed by *Copernicus* (Snow and Morton 1976), except that in α Cyg the typical P Cygni emission component at positive velocities is suppressed by the presence of a strong underlying photospheric absorption wing. The profiles indicate that the wind from α Cyg is accelerated to a terminal velocity at the stellar surface. The many Fe II resonance lines in the BUSS spectra of α Cyg have similar profiles to those of Mg II, but in addition they show the presence of two absorption components at -125 and -195 km s^{-1}. This last component was present only during the observation of 1976 May 20 and not in 1976 September 17.

The spectrum of β Ori observed in 1976 September showed two components of the Mg II resonance lines shifted by -190 km s^{-1}. These components were not present during previous high-resolution observations in 1974 (Boksenberg *et al.* 1975) or 1975 (Selvelli, Crivellari, and Stalio 1976). Selvelli *et al.* had found that the wind in β Ori is accelerated to 530 km s^{-1} and that the degree of ionization is high. Consequently, the appearance of the shifted Mg II components indicates that significant density variations occur in the stellar wind, which results in concentrations of low-ionization species.

The Mg II lines in η Leo and α Lyr do not show the presence of mass loss as the lines are symmetric and not shifted. However, Kondo, Morgan, and Modisette (1976) found shortward-shifted excess absorption in the spectrum of η Leo, observed during a previous BUSS flight.

* Space Research Laboratory, The Astronomical Institute, Utrecht.

† NASA Goddard Space Flight Center.

‡ Houston Baptist University.

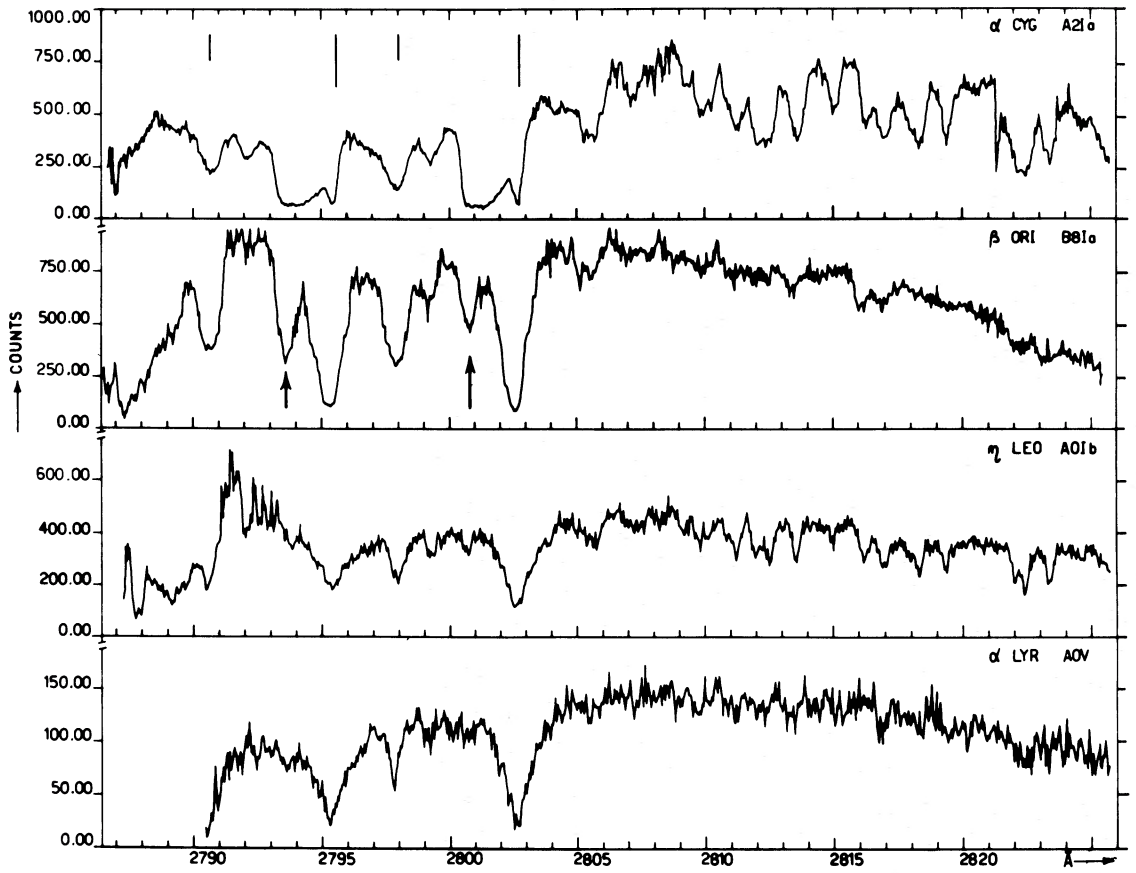

FIG. 1.—BUSS spectra of α Cyg, β Ori, η Leo, and α Lyr in the region 2787–2825 Å. The ordinate gives the flux in an arbitrary linear scale. The laboratory wavelengths of the Mg II resonance lines (*long vertical lines*) and the subordinate lines (*short vertical lines*) are indicated. The position of two extra components of the Mg II resonance lines in β Ori is indicated by arrows. These components were absent in previous observations of the spectrum.

These observations indicate that the mass loss from late-B and A-type supergiants is variable, with the occurrence of occasional stellar "puffs" superposed on a more or less regular wind. The visual spectra of both α Cyg and β Ori show irregular short time variability in Hα and in addition, α Cyg is pulsating nonradially (Lucy 1976). A possible correlation between the wind variations and the photospheric variations may give a clue to the origin of the stellar "puffs."

A more extended study of these stars and the mass-loss rates is published by Lamers, Stalio, and Kondo (1978).

III. THE Mg II RESONANCE DOUBLET EMISSION LINES NEAR 2800 Å IN BETELGEUSE (M2 Iab)

The Mg II resonance doublet lines are observed basically as two prominent emission lines with a central self-reversal. However, the 2795 component is pronouncedly asymmetric, while the 2802 component is reasonably symmetric; see Figure 2. This was first reported by Kondo *et al.* (1972) and was later confirmed by Kondo, Morgan, and Modisette (1975) and by Bernat and Lambert (1976). Following the suggestion by Herbig, the asymmetry has been attributed to the selective absorption by an Fe I line located at 2795.006 Å which gives rise to the fluorescence of the Fe I line at λ4204 and λ4307 (Spitzer 1939). The higher resolution attained in the current observations enables one to estimate the effect of the Fe I absorption more reliably than in the previous estimate by Modisette, Nicholas, and Kondo (1973). It is noted that the selective absorption in Figure 2 tends to favor Fe I, although Mn I may also be contributing.

In evaluating the equivalent width of the selective absorption, we employed the technique used by Modisette *et al.* It is basically a Gaussian curve fitting technique with several constraints, which results in a reasonably unique solution. The equivalent width of the Fe I absorption is 0.68 Å and the center is shifted by -12 km s^{-1} with respect to the reference frame of the Mg II emission components. If measured in the frame of the center of the self-reversal of the Mg II lines, the Fe I absorption is shifted by -17 km s^{-1} as the self-reversal is shifted $+5$ km s^{-1} with respect to the emission-line center. The width of the Fe I absorption line would be about 50 km s^{-1} if it were due entirely to turbulence.

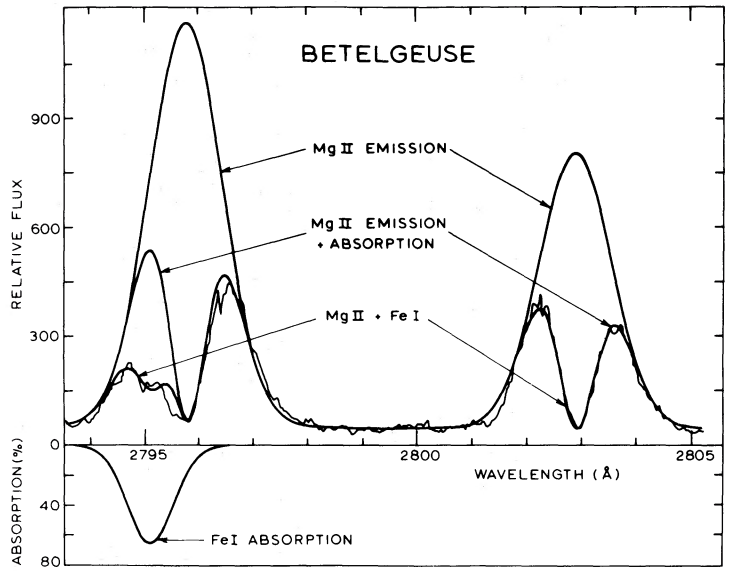

FIG. 2.—Analysis of the Mg II emission lines of α Ori in terms of a cool shell above a warmer chromosphere

The turbulence velocity in the Fe I absorbing shell has been estimated to be in the range of some 10 to 20 km s^{-1} by various workers. The broadness of the Fe I absorption profile indicates a large optical depth of the absorbing layer. The large width may also be due, in part, to the imperfection of the technique used.

IV. BE AND SHELL-TYPE STARS

Unexpected spectral features are present in the mid-UV spectra of Be stars and shell stars. Four stars of this group were observed during BUSS VIII: γ Cas (B0.5 IVel), φ Per (B2 Ve4p), υ Cyg (B2 Vel), and ζ Tau (B4 IIIp) (spectral types of Lesh 1968). Specimens of part of the spectra of three stars are shown in Figure 3. Of these stars φ Per has perhaps the most interesting spectrum, showing strong asymmetric absorption lines with short-wavelength wings extending 2.5 Å from the line center at three Fe III transitions of the same multiplet (UV 48 at λλ2078.99, 2068.24, and 2061.55) whose lower level is a low-lying metastable state.

The spectra of these four stars are quite different from each other. Both φ Per and υ Cyg show emission lobes to the Mg II doublet lines, while ζ Tau and γ Cas do not. Also γ Cas shows no absorption in the Fe III lines. The spectra of γ Cas and ζ Tau do not show any emission line in the mid-UV and do not show the λ2842.6 line, although ζ Tau has changed markedly since the last high-resolution observations were obtained (Morgan, Kondo, and Modisette 1977). In particular, the Mg II subordinate lines are now nearly absent (the equivalent width of the λ2798 has a value of only 150 mÅ at best), and the resonance lines are very strong and sharp, which suggests an important nonphotospheric component. The noninterstellar component is shifted significantly (at least 50 km s^{-1}) toward long wavelengths, which may be evidence that at the time of the observation a new infall of shell material was occurring (Delplace and van der Hucht 1978).

V. EMISSION LINES IN THE BUSS SPECTRA OF GIANTS AND SUPERGIANTS

Ground-based spectral observations in the range 3150–3000 Å of M-type giants and supergiants show emission lines of Fe II (Herzberg 1948) which are not observed in K-type giants and supergiants (Boesgaard and Boesgaard 1976).

In the ultraviolet wavelength region observed by BUSS, notably the region 2650–3100 Å, not only Fe II emission lines but also Fe I emission lines have been found. These occur not only in the spectra of the M supergiants α Ori and α Sco, but also in the spectra of α Tau (K5 III) and α Boo (K2 IIIp). The lines are shifted to longer wavelengths by about +20 K m^{-1}. In the spectra of the four mentioned stars, 80 different emission lines have been identified (van der Hucht *et al.* 1979*b*). Figure 4 shows an example of these observations. Intensity ratios of Fe I and Fe II lines will allow an analysis of the outer layers of these late type stars.

VI. THE SPECTRUM OF α SCORPI (M1.5 Iab + B2.5 V)

The primary of the Antares system, α^1 Sco, observed in the BUSS VII flight, has the same spectral type as α Ori (Morgan and Keenan 1973), i.e., M1.5 Iab. The BUSS observations show chromospheric emission lines for both these M-type supergiants, but no photospheric absorption spectrum (for exposure times, see Paper I).

The secondary of Antares, α^2 Sco, which has a spectral type B2.5 V (Garrison 1967), is 4 mag fainter than α^1 Sco, and at an angular distance of 2″.9. It is

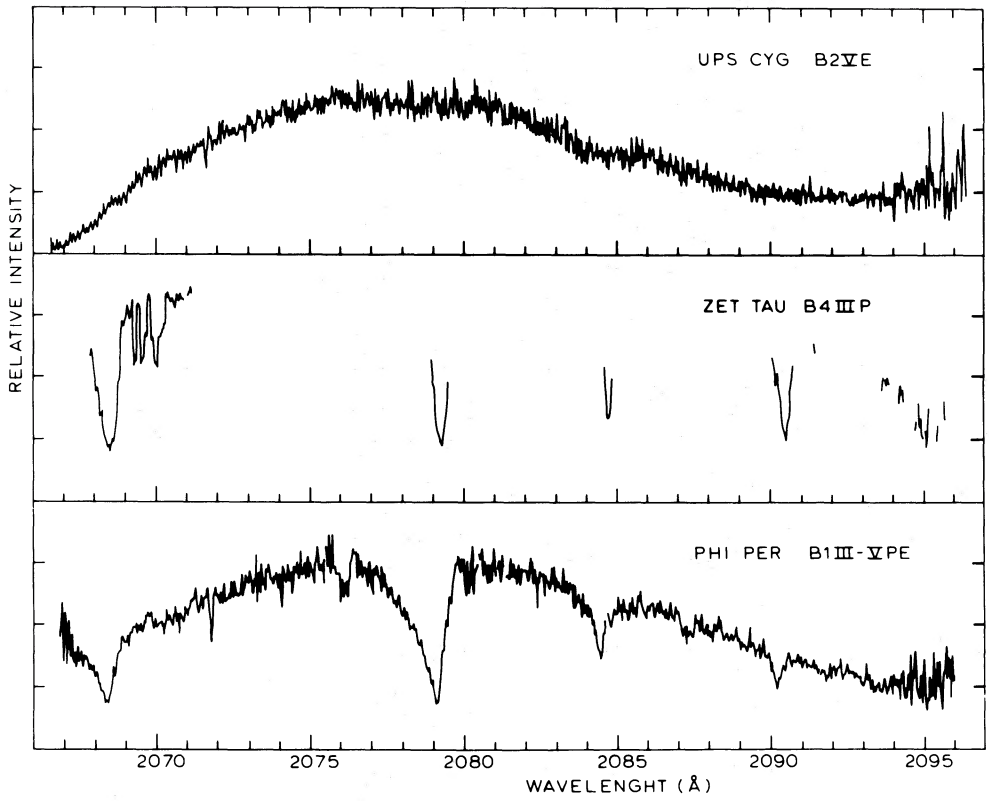

FIG. 3*a*

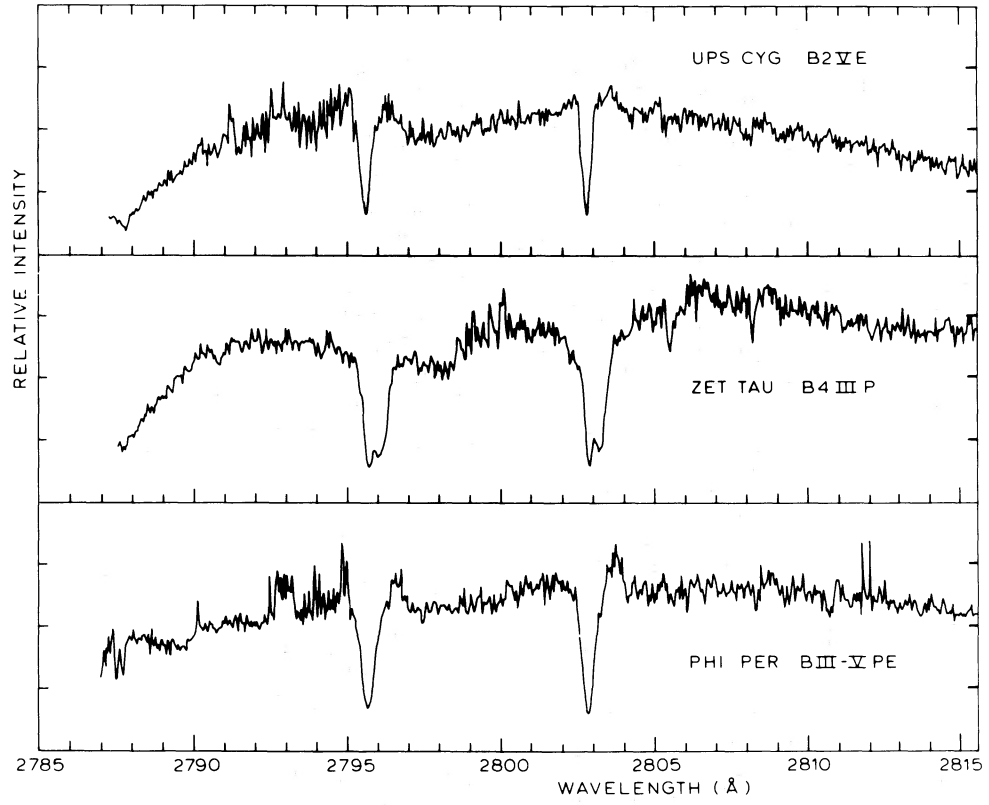

FIG. 3*b*

FIG. 3.—Spectra of the Be stars υ Cyg, ζ Tau, and ϕ Per in the spectral ranges (*a*) 2070–2095 Å and (*b*) 2785–2815 Å

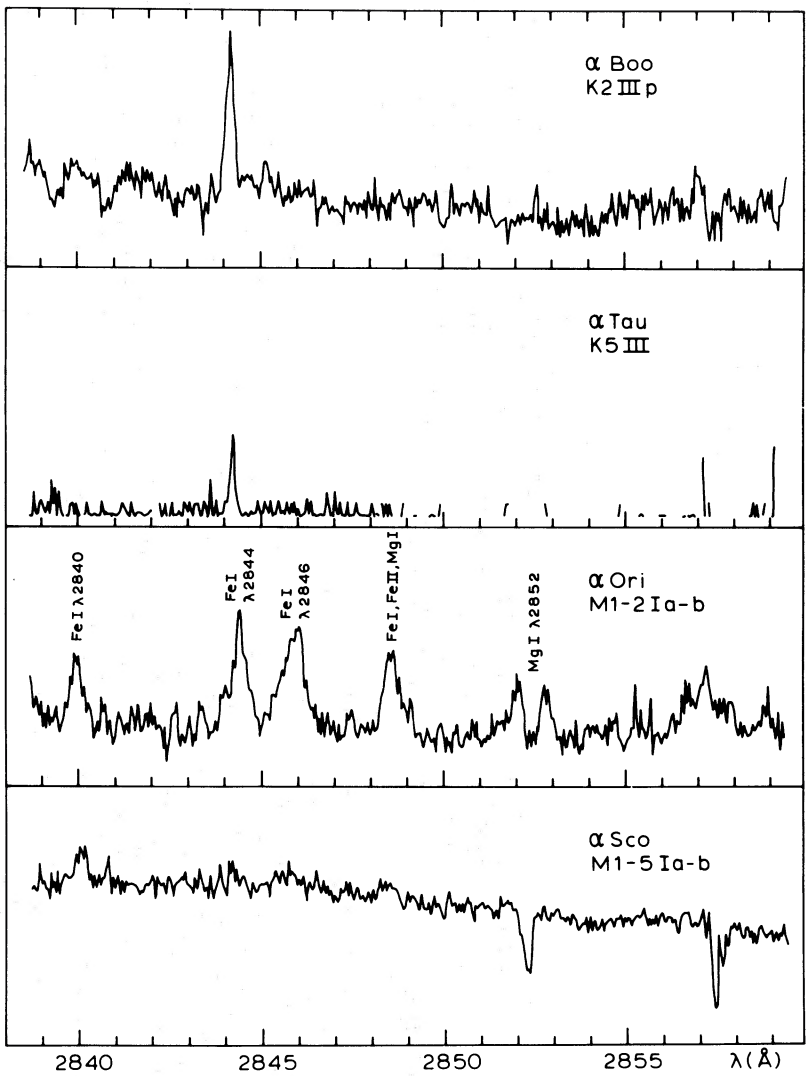

FIG. 4.—Emission lines of Fe I and Fe II in K-type giants and M-type supergiants

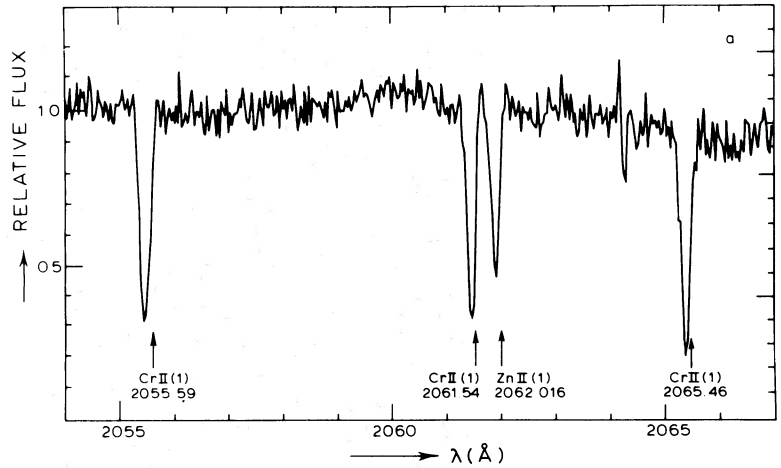

FIG. 5.—Circumstellar absorption lines of Cr II near 2060 Å in the spectrum of α Sco

thus visible within the circular 1′ entrance aperture of the BUSS spectrograph, which results in a composite spectrum. The 45 minute integration time was quite adequate to obtain also a good signal of the B star's photospheric spectrum.

M-type giants and supergiants are known to have very extended circumstellar (CS) shells. In the case of α^1 Sco, the shell extends to at least the distance of α^2 Sco (Kudritzki and Reimers 1978). Consequently the shell features are observed in absorption in the spectrum of the B star. In the BUSS UV spectrum of Antares, discussed by van der Hucht, Bernat, and Kondo (1979), shortward-shifted CS absorption lines of Cr II (UV 1) and Ni II (UV 11, 12, 13, and 14) have been identified, as well as CS contributions to absorption lines of Mg I, Mg II, Fe II, and Zn II. Figure 5 shows the Cr II CS absorption lines. They have a FWHM of ~ 0.2 Å and are shortward-shifted over -0.9 Å, corresponding to a radial velocity in the line of sight to α^2 Sco of -13 km s^{-1}. This observation allows the determination of the abundance of the various ions in the CS shell of Antares, and its mass loss.

The observations of α Sco also show, in addition to the Fe I and Fe II emission lines, emission lines of Fe III (UV 48) at $\lambda\lambda$2078.99 and 2068.24. The presence of the B star in the circumstellar shell of α^1 Sco may be the cause of these emission lines.

REFERENCES

Allen, C. W. 1973, *Astrophysical Quantities* (3d ed.; London: Athlone Press).
Bernat, A. P. 1977*a*, *Ap. J.*, **213**, 756.
———. 1977*b*, private communication.
Bernat, A. P., and Lambert, D. L. 1976, *Ap. J.*, **204**, 830.
Boesgaard, A., and Boesgaard, H. 1976, *Ap. J.*, **205**, 448.
Boksenberg, A., Kirkham, B., Towlson, W. A., Venis, T. E., Bates, B., Carson, P. P. D., and Courts, G. R. 1975, *Space Res.*, **14**, 533.
Bruhweiler, F. C., Morgan, T. H., and van der Hucht, K. A. 1978, *Ap. J. (Letters)*, **225**, L71.
Delplace, A. M., and van der Hucht, K. A. 1978, *Astr. Ap.*, **67**, 399.
Garrison, R. F. 1967, *Ap. J.*, **147**, 1010.
Herzberg, G. 1948, *Ap. J.*, **107**, 94.
Kondo, Y., de Jager, C., Hoekstra, R., van der Hucht, K. A., Kamperman, T. M., Lamers, H. J. G. L. M., Modisette, J. L., and Morgan, T. H. 1979, *Ap. J.*, **230**, 526.
Kondo, Y., Giuli, R. T., Modisette, J. L., and Rydgren, R. E. 1972, *Ap. J.*, **176**, 153.
Kondo, Y., Morgan, T. H., and Modisette, J. L. 1975, *Ap. J. (Letters)*, **198**, L37.
———. 1976, *Ap. J.*, **209**, 489.
Kudritzki, R. P., and Reimers, D. 1978, *Astr. Ap.*, **70**, 227.
Lamers, H. J. G. L. M., Stalio, R., and Kondo, Y. 1978, *Ap. J.*, **223**, 207.
Lesh, J. R. 1968, *Ap. J. Suppl.*, **17**, 371.
Lucy, L. B. 1976, *Ap. J.*, **206**, 499.
Modisette, J. L., Nicholas, R. E., and Kondo, Y. 1973, *Ap. J.*, **186**, 219.
Morgan, W. W., and Keenan, P. C. 1973, *Ann. Rev. Astr. Ap.*, **11**, 29.
Morgan, T. H., Kondo, Y., and Modisette, J. L. 1977, *Ap. J.*, **216**, 457.
Selvelli, P. L., Crivellari, L., and Stalio, R. 1977, *Astr. Ap. Suppl.*, **27**, 1.
Snow, T. P., and Marlborough, J. M. 1976, *Ap. J. (Letters)*, **203**, L87.
Snow, T. P., and Morton, D. C. 1976, *Ap. J. Suppl.*, **32**, 429.
Spitzer, L. 1939, *Ap. J.*, **90**, 494.
van der Hucht, K. A., Bernat, A. P., and Kondo, Y. 1979, *Astr. Ap.*, submitted.
van der Hucht, K. A., Stencel, R. E., Haisch, B. M., and Kondo, Y. 1979, *Astr. Ap. Suppl.*, in press.

C. DE JAGER, R. HOEKSTRA, T. M. KAMPERMAN, H. J. G. L. M. LAMERS, and K. A. VAN DER HUCHT: Space Research Laboratory, Beneluxlaan 21, Utrecht, The Netherlands

Y. KONDO: Code 685, NASA Goddard Space Flight Center, Greenbelt, MD 20771

J. L. MODISETTE and T. H. MORGAN: Houston Baptist University, 7502 Fondren Road, Houston, TX 77074